

THERMAL CONTINUA OF AGN DISKS: ATMOSPHERES, LYMAN EDGES, AND SOFT X-RAYS

H. H. Coleman

Astronomy Department, The University of Texas at Austin

and

G. A. Shields

Astronomy Department, The University of Texas at Austin

RESUMEN

Se calcularon los continuos espectrales en el ultravioleta y rayos x suaves para discos delgados dominados por presión de radiación usando los modelos de atmósferas caracterizados por bajas gravedades efectivas. Se incorporaron en los cálculos efectos relativistas y de desviaciones de Equilibrio Termodinámico Local. De acuerdo con las observaciones, se encuentra que los bordes de Lyman son insignificantes para un amplio intervalo de masas, tasas de acreción y ángulos de vista. El intervalo de las luminosidades en rayos x suaves es consistente con las observaciones, si suponemos que los discos orbitan alrededor de hoyos negros en rotación máxima.

ABSTRACT

Ultraviolet and soft X-ray continuum spectra are calculated for thin, radiation-pressure-dominated disks using model atmospheres characterized by appropriately low effective gravities. Relativistic and non-LTE effects are incorporated in the calculations. In agreement with observations, Lyman edges are found to be insignificant over a wide range of masses, accretion rates, and viewing angles. The range of soft X-ray luminosities is consistent with observations if the disks are assumed to orbit maximally rotating black holes.

Key words: **ACCRETION, ACCRETION DISKS — GALAXIES: ACTIVE — X-RAYS: GALAXIES**

1. Introduction

Thin accretion disks have long been favored as the sources of the “Blue Bump” optical-ultraviolet emission feature characteristic of the spectra of active galactic nuclei (AGN) (Shakura & Sunyaev 1973; Novikov & Thorne 1973; Shields 1978). AGN disks have been modeled as blackbody emitters (Malkan & Sargent 1982; Malkan 1983), as blackbody emitters modified by the effects of electron scattering opacity (Czerny & Elvis 1987; Wandel & Petrosian 1988; Laor & Netzer 1989; Laor, Netzer, & Piran 1990), and as superpositions of stellar atmospheres (Kolykhalov & Sunyaev 1984; Sun & Malkan 1986). Non-LTE calculations have been carried out for the EUV continuum of constant-density disks by Ross, Fabian, & Mineshige (1992). Detailed LTE atmospheric models were constructed for a limited range of disk parameters by Störzer (1991).

Important questions remain. The lack of observed Lyman edges in AGN spectra (Antonucci, Kinney, & Ford 1989) is not well reproduced by most models and has been used as an argument against thin disks as the source of the Blue Bump. If the commonly observed soft X-ray emission in AGN (Turner & Pounds 1989) is the high-energy extension of the Blue Bump, it constitutes a further problem for current disk models (Laor & Netzer 1989).

Both the Lyman edge and the soft X-ray extent of disk emission depend critically on the treatment of the disk atmosphere and the inclusion of non-LTE population levels in radiative transfer calculations. These issues are discussed in the next section. Section 3 outlines the atmospheric modeling and spectral calculations, and results are presented in Section 4.

2. Basics

The key to understanding AGN disk continua is the realization that the photospheres have extremely small effective gravities, g_{eff} . The innermost parts of the disk, where ultraviolet and soft X-ray emission originates, are supported by radiation pressure. From the disk midplane to the base of the photosphere, a fine balance exists between the upward acceleration, g_{rad} , due to the radiation flux, and the vertical component of gravity, g_z . Thus, while g_z nominally is comparable to O-star gravities ($\sim 10^4 \text{ cm s}^{-2}$), $g_{eff} = g_z - g_{rad}$ is smaller by two or three orders of magnitude, commonly ranging from a few hundred to less than one cm s^{-2} . This has profound effects on the nature of the continuum emission.

The photospheric gas pressure scale height, h_{gas} , varies inversely with the effective gravity: $h_{gas} = c_s^2/g_{eff}$, where c_s is the gas pressure sound speed. Since the density ρ at the base of the photosphere is determined by $\tau \sim \kappa_{es}\rho h_{gas} \sim 1$, the photospheric density varies inversely with h_{gas} . (Here τ is the optical depth measured from the surface of the photosphere downward and κ_{es} is the opacity due to electron scattering, the dominant opacity source in these hot photospheres.) Low effective gravities result in large gas pressure scale heights and small photospheric densities.

Low densities influence the continuum shape by reducing absorption opacities, in particular, the bound-free opacity responsible for the Lyman edge. Not only is κ_{bf} proportional to density, but, at low densities and high effective temperatures, non-LTE effects become important, further depopulating the $n = 1$ level of hydrogen (and, in some cases, of ionized helium as well). Resulting absorption edges are reduced and, if $\kappa_{bf} \ll \kappa_{es}$, small emission edges may appear. Reduction of the He II Lyman edge opacity permits the continuum to extend to soft X-ray wavelengths.

The observed spectrum combines weak absorption or emission edges from inner, hot radii with stronger absorption edges from cooler, outer radii. Flux levels are lower at large radii, but the emitting area is greater. The situation is further complicated by relativistic effects. Not only do Doppler shifts smear spectral features, but, particularly for disks in Kerr metrics, radiation from small radii is Doppler-beamed into the disk's equatorial plane. Both the character of edges and the hardness of the observed continuum depend, not only on the physics of the disk atmosphere, but on the inclination of the disk with respect to the observer and the rotation of the central black hole.

3. Procedure

Given the accretion rate and the mass and rotation of the black hole, spectra are calculated for each of about a dozen radii. A vertical density profile for the disk and photosphere is calculated by integrating the equations of hydrostatic equilibrium and energy generation along with a simplified radiative transfer equation from the disk midplane to the top of the atmosphere. A temperature profile corresponding to this density structure is derived with the aid of a simple LTE atmosphere code. The resulting density and temperature stratifications are used by a non-LTE radiative transfer code (supplied by Dietmar Kunze of the Institut für Astronomie und Astrophysik der Universität München) to compute the emergent local spectrum. A propagation code which takes relativistic effects into account (Laor, Netzer, & Piran 1990) integrates the disk emission, producing the observed spectrum as a function of disk inclination.

4. Results

A series of models has been produced for both Schwarzschild (nonrotating) and Kerr (maximally rotating) black holes. Eddington ratios range from 6×10^{-4} to 0.3, a limit beyond which the thin disk approximation is no longer valid. Disk bolometric luminosities range from 10^{43} to $10^{48} \text{ erg s}^{-1}$, and masses are included from $10^6 M_\odot$ to nearly $10^{11} M_\odot$.

A typical sequence of model spectra is shown in Fig.1. At constant Eddington ratio, L/L_{Edd} , increasing the maximum disk temperature, T_{max} , diminishes the Lyman edge and greatly enhances short wavelength emission. Even in cases with strongly absorbing Lyman edges, relativistic smearing smoothes the edge from a discontinuity into a continuum slope change. Generally, an absorption feature remains at the He II $\lambda 228\text{\AA}$ edge, though in the hottest models this edge, too, disappears.

For a viewing angle of 60° , Kerr and Schwarzschild disks with equivalent T_{max} and Eddington ratios have similar Lyman edges. Continua of low temperature disks have strong absorption edges. As the temperature is increased at constant Eddington ratio, the absorption edges diminish, passing into moderate emission. At even higher temperatures, the edges return again to zero.

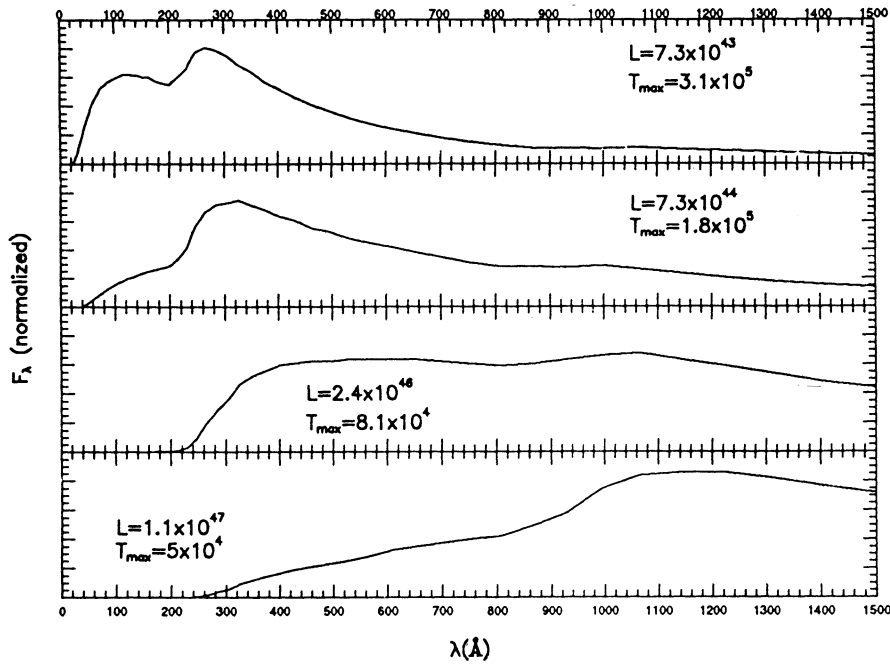


Fig. 1. Continua of Kerr disks, $L/L_{Edd} = 0.06$, $\cos(\theta_{obs}) = 0.9$ (nearly face-on)

Lyman edges vary with increasing Eddington ratio in the same way they respond to increasing T_{max} . At fixed T_{max} , absorption edges become weaker as L/L_{Edd} increases and photospheric densities become smaller.

The disk models produce soft X-rays at luminosities comparable to those suggested by currently available observations. At fixed Eddington ratio, disks become cooler and larger with increasing bolometric luminosity, so that the X-ray flux drops while the emitting region increases in size. Therefore, a maximum X-ray luminosity exists for the disk models (see Fig.2). For the Schwarzschild metric, that maximum is $\sim 10^{44} \text{ erg s}^{-1}$, a value exceeded by several observed objects. The maximum X-ray luminosity of Kerr disks is just over $10^{46} \text{ erg s}^{-1}$, consistent with available data.

An object for which continuum observations are available at rest wavelengths significantly less than 912 Å is the extremely luminous source HS 1700+6416 (Reimers *et al.* 1989). The spectrum is strongly modified by intervening absorption, but the estimated intrinsic continuum, extending to 300 Å, has been cited as evidence that the emission cannot arise in a thermal disk. We have achieved a close fit to this continuum with a model using a Kerr hole of $6.8 \times 10^{10} M_{\odot}$ and $\dot{M} = 153 M_{\odot} \text{ yr}^{-1}$ and a viewing angle near the equatorial plane so that relativistic beaming boosts the high frequency flux.

5. Conclusions

Our work indicates that the lack of conspicuous observed Lyman edges does not rule out accretion disks as the source of the Blue Bump. Weak edges, made even more inconspicuous by relativistic smearing, are expected over a wide range of disk parameters and viewing angles. Kerr disks produce a given luminosity at a higher temperature than do the corresponding Schwarzschild disks. Kerr disks are thus preferred as the source of continua with weak Lyman edges.

Soft X-rays are produced by Kerr disks at luminosities which are in quantitative agreement with current observations. The predicted maximum soft X-ray luminosity for Kerr disks places a testable constraint on such objects as sources of soft X-ray excesses in AGN.

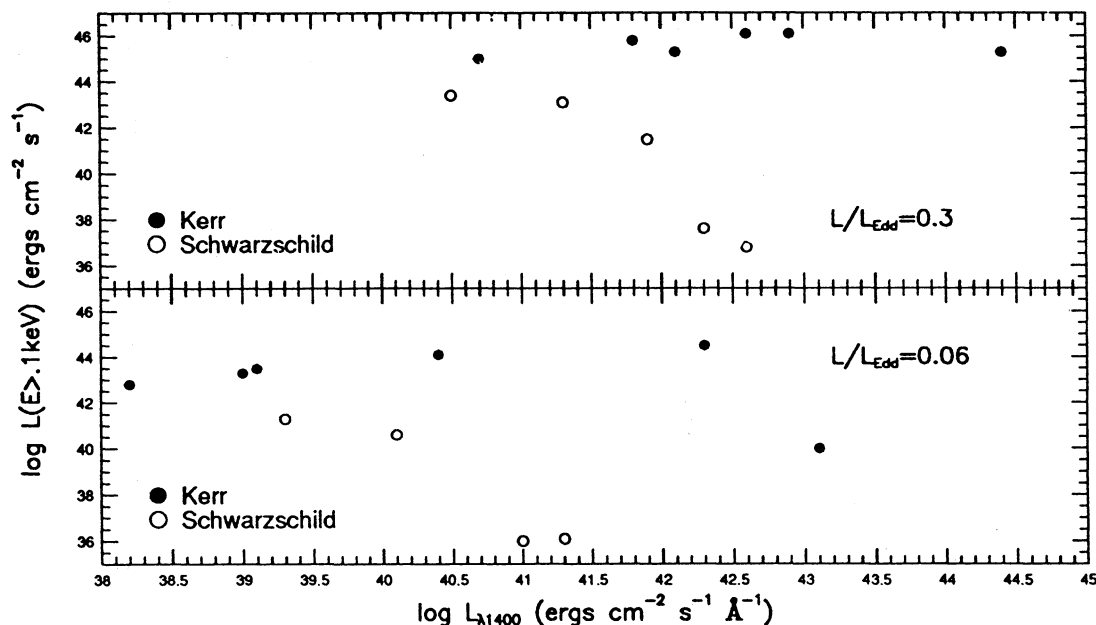


Fig. 2. Soft X-ray vs ultraviolet luminosities

The authors gratefully acknowledge the support of NASA Training Grant NGT 50659 and NASA Grant NAGW-1807.

REFERENCES

- Antonucci, R. R. J., Kinney, A. L., & Ford, H. C. 1989, *ApJ*, 342, 64
 Czerny, B., & Elvis, M. 1987, *ApJ*, 321, 305
 Kolykhalov, P. I., & Sunyaev, R. A. 1984, *Adv. Sp. Res.*, 3, 249
 Laor, A., & Netzer, H. 1989, *MNRAS*, 238, 897
 Laor, A., Netzer, H., & Piran, T. 1990, *MNRAS*, 242, 560
 Malkan, M. A. 1983, *ApJ*, 268, 582
 Novikov, I. D., & Thorne, K. S. 1973, in *Black Holes*, eds. C. DeWitt & B. S. DeWitt (New York: Gordon and Breach), p.343
 Reimers, D., Clavel, J., Groote, D., Engels, D., Hagen, H. J., Naylor, T., Wamsteker, W., & Hopp, U. 1989 *AA*, 218, 71
 Ross, R. R., Fabian, A. C., & Mineshige, S. 1992, *MNRAS*, 258, 189
 Shakura, N. I., & Sunyaev, R. A. 1973, *A&A*, 24, 337
 Shields, G. A. 1978, *Nature*, 272, 706
 Störzer, H. 1991, Dissertation, Universität Heidelberg
 Sun, W.-H., & Malkan, M. A. 1986, in *Astrophysical Jets and Their Engines*, ed. W. Kundt (Dordrecht: Reidel) p.125
 Turner, T. J., & Pounds, K. A. 1989, *MNRAS*, 240, 833
 Wandel, A., & Petrosian, V. 1988, *ApJ*, 329, L11.

Howard H. Coleman and Gregory A. Shields: University of Texas at Austin, Astronomy Dept., Austin, TX 78712-1083, U.S.A.